Pergamon

Int. J. Heat Mass Transfer. Vol. 39, No. 18, pp. 3813–3822, 1996

0017–9310/96 $15.00 + 0.00

PII: S0017–9310(96)00061–0

Calculation of wall heat transfer in pipe-expansion turbulent flows

W. D. HSIEH and K. C. CHANG†

Institute of Aeronautics and Astronautics, National Cheng-Kung University, Tainan, Taiwan, Republic of China

(*Received* 10 *May* 1995 *and in final form* 1 *February* 1996)

Abstract—A new modified low-Reynolds-number k-ε turbulence [Chang, Hsieh and Chen (CHC)] model, which possesses the proper near-wall limiting behaviors and is free of the singular defect occurring near the reattachment point when applied to separated flows, is examined for use in wall heat transfer problems in flow with pipe expansion geometry. Another eight low-Reynolds-number k-ε models, found in open literature, are also examined in this study. Attention is specifically focused on the flow region surrounding the reattachment point. Comparative results show that only the CHC model and the model developed by Abe *et al.* [Abe, Kondoh and Nagano (AKN model)] can yield satisfactory distributions of the Nusselt number along the wall. However, the CHC model adopted the same model constants as conventionally used for the standard k-ε model. Thus, the CHC model is more universal than the AKN model. Copyright © 1996 Elsevier Science Ltd.

INTRODUCTION

Turbulent flows downstream from backward facing steps or axisymmetric pipe expansions are encountered in many practical engineering applications such as combustors, nuclear reactors, heat exchangers and electronic circuitry cooling systems. The processes of the separation and reattachment of the turbulent shear layer not only determine the flow field structure, but also influence the mechanism of heat and mass transfer. In particular, near the reattachment region, heat and mass transfer rates are enhanced up to several times and decrease gradually until they equal to the typical values of ordinary boundary layer flows. Therefore, the accurate predictions of this augmentation and its associated thermal loads are important to the development of more efficient and safer devices.

Most of the previous studies concentrated on the predictions of the cold flow cases in computing turbulent separated flows through backward facing steps or axisymmetric pipe expansions. Moreover, the emphases of these studies were usually placed on the main flow regions (not in the near-wall regions), although some studies adopted near-wall turbulence models in their simulations. In practice, the prediction of the flow far from the wall generally remains unaffected by the choice of near-wall turbulence model. The local heat transfer prediction, however, is critically dependent on the employed near-wall turbulence model. For some physical problems, such as the flows in this kind of geometries, the accurate prediction of the flow field in the near-wall region is a prerequisite for the attainment of reliable wall heat transfer solutions. Accordingly, low-Reynolds-number versions of turbulence models seem to be necessary for the accurate prediction of these types of flows with wall heat transfer, especially in the region neighboring the reattachment points (hot spots). Attention is placed on axisymmetric pipe expansion flows in this study.

In the past one and a half decades, some researchers have attempted to model convective recirculating heat transfer flows for pipe expansion. Chieng and Launder [1] numerically studied the heat transfer problem in the pipe expansion geometry through both the standard (original) k-ε model incorporated with wall functions and its low-Reynolds-number version. The prediction obtained with the standard k-ε model was generally in fair agreement with the experimental data. However, the predicted location of the maximum Nusselt number failed to agree with the measured data. Furthermore, use of the low-Reynolds-number k-ε model resulted in predicted wall heat transfer rates which were about five times the actual value in the vicinity of the reattachment point. Chieng and Launder [1] argued that this was because the ε equation under diffusion-dominated conditions yielded unacceptably large length scales in the regions close to the wall. Amano [2, 3] repeated the test cases of Chieng and Launder [1] using multiple-layer wall functions and achieved some improvements over the work of the previous authors. To obtain accurate results in both the recirculating and developing flow regions, Gooray *et al.* [4] devised a two-pass procedure combining wall functions and the low-Reynolds-number version of the k-ε model. Although the multi-layer models [2, 3] and the two-pass procedure [4] have generally resulted in improved predictions, their per-

† Author to whom correspondence should be addressed.

NOMENCLATURE

C_μ, C_1, C_2 turbulence model constants
f_μ, f_1, f_2 turbulence model functions
D diameter of pipe downstream of expansion or extra source term in k equation
d diameter of pipe upstream of expansion
E extra source term in ε equation
G_k production term of k
k turbulent kinetic energy
Nu Nusselt number based on the diameter of pipe downstream of expansion
Nu_{fd} Nusselt number determined by the Dittus–Boelter equation, $Nu_{fd} = 0.023Re^{0.8}Pr^{0.4}$
p mean pressure
R radius of pipe downstream of expansion
Re Reynolds number
r radial coordinate
S_ϕ general source term
T temperature
T_i, T_w temperatures at inlet and wall, respectively
T_k Kolmogorov time scale
u, v mean axial and radial velocity components, respectively
u_c mean axial velocity at centerline
u_*, u_τ Kolmogorov velocity scale and friction velocity, respectively
x axial coordinate
y, y^+ normal and dimensionless distances from the wall, respectively
y^* dimensionless distance from the wall, see equation (5).

Greek symbols
Γ_ϕ turbulent diffusion coefficient
ε dissipation rate of turbulent kinetic energy
μ, μ_t, μ_{eff} molecular, eddy and effective viscosities, respectively
ν, ν_t molecular and eddy kinematic viscosities, respectively
ρ density
σ_k, σ_ε turbulent Prandtl numbers for diffusion of k and ε, respectively
σ_l, σ_t molecular and turbulent Prandtl number for diffusion of temperature, respectively
τ_w wall shear stress
θ general dependent variable.

Superscripts
$'$ fluctuation
$\bar{}$ Reynolds averaging.

formances are not always satisfactory. Prud'homme and Elgobashi [5] studied the heat transfer problem with the flow in pipe expansion geometry using a full Reynolds stress model (RSM) to close the time-averaged Navier–Stokes equations with an algebraic model for thermal flows. Their models accounted for the low Reynolds number effects in the wall region and thus avoided use of conventional wall functions. The predicted Nusselt number distribution was in satisfactory agreement with the measurements.

Yap [6] also computed the heat transfer problem in a pipe expansion geometry with a condition of uniform wall temperature using the algebraic stress model (ASM) and the k-ε model incorporated wall functions. His predictions, however, were found to have serious shortcomings. When the low-Reynolds-number k-ε was used with a fine grid mesh near the wall, the predicted peak values of the wall heat transfer rates were about five times higher than the experimental values. This situation was the same as that of Chieng and Launder [1]. However, after introduction of a wall-damping term into the ε equation by Yap [6], the predicted wall heat transfer rates were in good agreement with the experimental values. When the ASM was used instead of the k-ε model in the outer region, further improvements were made in the predictions of the heat transfer rate. Yap [6] concluded that computations with the ASM/low-Reynolds-number k-ε model could yield predictions which agreed with experimental results, but the approach could not be applied universally [7, 8]. Furthermore, use of either the full RSM or the ASM greatly increases the computational complexity and time required for computations. As the order of the turbulence model increases, the number of empirical constants increases, and insufficient model assessments lead to less generality of those empirical constants. A general method for flow simulation must comprise both a physical model that reflects the true nature of the flow and an efficient mathematical apparatus that permits accurate and yet economical calculations. It is, so far, not clear whether the higher-order closure models are more valuable than the two-equation models. The scope of this work is restricted to separate flows in a sudden-expansion pipe without the swirl effect. The two-equation models are reportedly able to describe, to a certain extent, the turbulent motion in this kind of flow [9]. Recently, the application of nonlinear (or anistropic) eddy-viscosity near-wall turbulence models to heat transfer problems has been widely investigated [10–12]. In this work, our interest is specifically placed on the flow region in the neighborhood of

the reattachment point. For the sake of brevity, the conventional two-equation models, instead of the ones with anisotropic representation of the eddy viscosity, are to be discussed here.

Patel *et al.* [13] made an extensive review of the low-Reynolds-number turbulence models developed before 1985 and concluded that none of the low-Reynolds-number k-ε models investigated were capable of predicting near-wall limiting behaviors. Significant advances have been made in recent years in the development of near-wall turbulence models. For example, Myong and Kasagi (MK model, [14]) as well as Nagano and Tagawa (NT model, [15]) took into account the near-wall limiting behaviors and yielded satisfactory predictions in the entire flow region of a straight pipe. However, application of these low-Reynolds-number k-ε turbulence models to the separated flow is subject to a singular difficulty occurring near the reattachment points. A detailed discussion of this singular difficulty is referred to in our previous work (CHC model, [16]). Recently, Yang and Shih (YS model, [17]) introduced the Kolmogorov time scale into the definition of eddy viscosity to account for the near-wall turbulent behavior, and their model function f_μ was expressed in terms of a 'frame invariant' parameter to avoid the singularity. However, their model has not been applied to the separated flows yet. Abe *et al.* (AKN model, [18]) adopted a new approach to develop a new low-Reynolds-number k-ε model, which can avoid the singularity and exhibit near-wall limiting behavior, as applied to a two-dimensional, isothermal, backward-facing step flow.

The objective of this study is first to examine the performance of six conventional low-Reynolds-number k-ε models developed by Launder and Sharma (LS model, [19]), Lam and Bremhorst (LB model, [20]), Chien (CH model, [21]), Nagano and Hishida (NH model, [22]), Myong and Kasagi (MK model, [14]) and Nagano and Tagawa (NT model, [15]), in addition to the two currently developed ones by Yang and Shih (YS model, [17]) and by Abe *et al.* (AKN model, [18]) in predicting nonisothermal flows in pipe expansions. Special emphasis will be placed on the capability to predict wall heat transfer near the reattachment point. Next, the modified low-Reynolds-number k-ε model developed previously by our group (CHC model, [16]) will be applied to the same heat transfer problems, and its performance will be compared to those of other models using the available data bases found in open literature. All investigated low-Reynolds-number k-ε models are summarized in Table 1.

LOW-REYNOLDS-NUMBER k-ε MODELS

The primary difference between the low-Reynolds-number k-ε models and the standard k-ε model is that the former introduce the model functions which account for the low-Reynolds-number effects in near-wall regions. Patel *et al.* [13] showed that the near-wall limiting conditions of turbulence quantities possess the following relationship:

$$-\overline{u'v'} \propto y^3, k \propto y^2, \nu_t \propto y^3, \varepsilon \to \varepsilon_w \text{ as } y \to 0, \quad (1)$$

where y denotes the neighboring distance from the wall. With the Prandtl–Kolmogorov relation, $\nu_t = C_\mu f_\mu k^2/\varepsilon$, and the model coefficient C_μ being a constant value of 0.09, the model function f_μ has to satisfy $f_\mu \propto y^{-1}$. A few low-Reynolds-number k-ε models developed lately have taken this requirement into account. For example, Myong and Kasagi (MK model, [14]) proposed the model function of f_μ in the form of

$$f_\mu = [1 - \exp(-y^+/70)](1 + 3.45/R_t^{1/2}), \quad (2)$$

where $R_t = k^2/\nu\varepsilon$. Working with the model developed previously by Nagano and Hishida [22] as a base, Nagano and Tagawa (NT model, [15]) improved the f_μ function

$$f_\mu = [1 - \exp(-y^+/26)]^2(1 + 4.1/R_t^{3/4}). \quad (3)$$

Very recently, Abe *et al.* [18] developed a new low-

Table 1. Summary of model functions

Model	f_μ	f_1	f_2
Standard	1.0	1.0	1.0
Launder–Sharma [19]	$\exp[-3.4/(1-R_t/50)^2]$	1.0	$1.0-0.3\exp(-R_t^2)$
Lam–Bremhorst [20]	$[1.0-\exp(-0.0165R_k)]^2(1+20.5/R_t)$	$1.0+(0.05/f_\mu)^3$	$1-0.3\exp(-R_t^2)$
Chien [21]	$1.0-\exp(-0.0115y^+)$	1.0	$1.0-0.22\exp(-R_t^2/36)$
Nagano–Hishida [22]	$[1.0-\exp(-y^+/26)]^2$	1.0	$1.0-0.3\exp(-R_t^2)$
Myong–Kasagi [14]	$[1.0-\exp(-y^+/70)](1+3.45/R_t^{1/2})$	1.0	$\{1.0-2/9\exp[-(R_t/6)^2]\}[1-\exp(-y^+/5)]^2$
Nagano–Tagawa [15]	$[1.0-\exp(-y^+/26)]^2(1+4.1/R_t^{3/4})$	1.0	$\{1.0-0.3\exp[-(R_t/6.5)^2]\}[1-\exp(-y^+/6)]^2$
Yang–Shih [17]	$[1.0-\exp(-1.5\times10^{-4}R_k - 5.0\times10^{-7}R_k^3 - 1.0\times10^{-10}R_k^{5\,1/2}$	1.0	1.0
Abe *et al.* [18]	$[1.0-\exp(-y^*/14)]^2\{1+5.0/R_t^{3/4}\exp[-(R_t/200)^2]\}$	1.0	$\{1.0-0.3\exp[-(R_t/6.5)^2]\}[1-\exp(-y^*/3.1)]^2$
Chang *et al.* [16]	$[1.0-\exp(-0.0215R_k)]^2(1+31.66/R_t^{5/4})$	1.0	$[1-0.01\exp(-R_t^2)][1-\exp(-0.0631R_k)]$

Reynolds-number k-ε model (AKN model which was modified from the NT model [15]) with the f_μ function in terms of the Kolmogorov velocity scale (u_ε) instead of the friction velocity (u_τ).

$$f_\mu = [1-\exp(-y^*/14)]^2\{1+5/R_t^{3/4} \times \exp[-(R_t/200)^2]\}, \quad (4)$$

where

$$y^* = u_\varepsilon y/\nu \quad (5)$$

$$u_\varepsilon = (\nu\varepsilon)^{1/4}. \quad (6)$$

Yang and Shih [17] argued that the turbulence time scale was given by k/ε away from the wall and by the Kolmogorov time scale near the wall since k/ε vanished near the wall due to the boundary condition on k. Thus, they defined the eddy viscosity in their low-Reynolds-number model (YS model) as

$$\mu_t = C_\mu f_\mu \rho k(k/\varepsilon + T_k) \quad (7)$$

in which Kolmogorov time scale is given by

$$T_k = C_k(\nu/\varepsilon)^{1/2}, \quad (8)$$

where C_k is a constant from 0.5 to 3.0 and was set to be unity in their study. The damping function is taken in terms of a 'frame invariant' parameter, R_k, which is defined by

$$R_k = \sqrt{k}y/\nu \quad (9)$$

and takes the following form:

$$f_\mu = [1-\exp(-1.5\times10^{-4}R_k - 5.0\times10^{-7}R_k^3 - 1.0\times10^{-10}R_k^5)]^{1/2}. \quad (10)$$

Note that $f_\mu \propto y$ as $y \to 0$ in the YS model [17] and this is not consistent with the proper near-wall limiting behavior as discussed before.

Although the model functions of f_μ developed lately, excluding that of the YS model, possess the near-wall limiting behavior of $f_\mu \propto y^{-1}$ as $y \to 0$, these model functions, with the exception of the YS and AKN models, still have a singular defect when applied to separated flows such as that in a sudden-expansion pipe [18]. This is because these turbulence models formulated their f_μ model functions in terms of wall shear stress (τ_w) as a parameter. It is known that the wall shear stress becomes close to zero as the reattachment point of the separated flow is approached. This, in turn, leads to a singular problem, that is, f_μ becomes zero regardless of y's value. This is physically impossible as was corroborated by several researchers [17, 18, 23, 24]. Another model function f_2 which appears in the source term of the ε equation (see Table 2) may have a similar difficulty for some of the low-Reynolds-number k-ε models which are summarized in Table 1.

In order to eliminate this singular difficulty, the new model functions of f_μ and f_2 in terms of the proper parameters were proposed in our previous work [16] to avoid the occurrence of singularity at the reattachment point as follows:

$$f_\mu = [1-\exp(-0.0215R_k)]^2(1+31.66/R_t^{5/4}) \quad (11)$$

$$f_2 = [1-\exp(-0.0631R_k)][1-0.01\exp(-R_t^2)]. \quad (12)$$

Note that the model functions appearing in equations (11) and (12) comply with the required near-wall limiting behaviors of $f_\mu \propto y^{-1}$ and $f_2 \propto y^2$ as y approaches zero value. All the model functions investigated in this work are summarized in Table 1. Among them, the LS and LB models are incapable of properly performing the near-wall limiting behavior, while the MK and NT models have a singularity in the neighborhood of the reattachment points. The CH and NH models, both of which inherently have the two aforementioned defects, were specially selected for this study to underscore the influence which combined effects have on the prediction accuracy. The AKN model [18] was free of the singularity and was able to reproduce the near-wall limiting behavior as

Table 2. Governing equations

θ	Γ_θ	S_θ
1	0	0
u	μ_{eff}	$-\frac{\partial p}{\partial x}+\frac{\partial}{\partial x}\left(\mu_{\text{eff}}\frac{\partial u}{\partial x}\right)+\frac{1}{r}\frac{\partial}{\partial r}\left(r\mu_{\text{eff}}\frac{\partial v}{\partial x}\right)$
v	μ_{eff}	$-\frac{\partial p}{\partial r}+\frac{\partial}{\partial x}\left(\mu_{\text{eff}}\frac{\partial u}{\partial r}\right)+\frac{1}{r}\frac{\partial}{\partial r}\left(r\mu_{\text{eff}}\frac{\partial v}{\partial r}\right)-2\mu_{\text{eff}}v/r^2$
k	$\mu+\mu_t/\sigma_k$	$G_k-\rho\varepsilon+D$
ε	$\mu+\mu_t/\sigma_\varepsilon$	$(C_1f_1G_k-C_2f_2\rho\varepsilon)\varepsilon/k+E$
T	$\mu/\sigma_1+\mu_t/\sigma_t$	0

$$G_K = \mu_t\left\{2\left[\left(\frac{\partial u}{\partial x}\right)^2+\left(\frac{\partial v}{\partial r}\right)^2+\left(\frac{u}{r}\right)^2\right]+\left(\frac{\partial u}{\partial x}+\frac{\partial v}{\partial r}\right)^2\right\}$$

$$\mu_t = \rho C_\mu f_\mu k^2/\varepsilon$$

$$\mu_{\text{eff}} = \mu+\mu_t$$

Table 3. Summary of model constants and functions appearing in Table 2

Model	D	E	$\varepsilon_w - B.C.$	C_μ	C_1	C_2	σ_k	σ_ε
Stanard	0	0	wall function	0.09	1.44	1.92	1.0	1.3
Launder–Sharma [19]	$-\frac{\mu}{2k}\left(\frac{\partial k}{\partial y}\right)^2$	$2\mu\nu_t\left(\frac{\partial^2 u}{\partial y^2}\right)^2$	0	0.09	1.44	1.92	1.0	1.3
Lam–Bremhorst [20]	0	0	$\frac{\partial \varepsilon}{\partial y} = 0$	0.09	1.44	1.92	1.0	1.3
Chien [21]	$-2\mu k/y^2$	$-2\mu\varepsilon e^{-0.5y^+}/y^2$	0	0.09	1.44	1.92	1.0	1.3
Nagano–Hishida [22]	$-\frac{\mu}{2k}\left(\frac{\partial k}{\partial y}\right)^2$	$(1-f_\mu)\mu\nu_t\left(\frac{\partial^2 u}{\partial y^2}\right)^2$	0	0.09	1.44	192	1.0	1.3
Myong–Kasagi [14]	0	0	$\varepsilon_w = \nu\left(\frac{\partial^2 k}{\partial y^2}\right)$	0.09	1.4	1.8	1.4	1.3
Nagano–Tagawa [15]	0	0	$\varepsilon_w = \nu\left(\frac{\partial^2 k}{\partial y^2}\right)$	0.09	1.45	1.9	1.4	1.3
Yang–Shih [17]	0	$\mu\nu_t\left(\frac{\partial^2 u}{\partial y^2}\right)^2$	$\varepsilon_w = \nu\left(\frac{\partial^2 k}{\partial y^2}\right)$	0.09	1.44	1.92	1.0	1.3
Abe *et al.* [18]	0	0	$\varepsilon_w = \nu\left(\frac{\partial^2 k}{\partial y^2}\right)$	0.09	1.5	1.9	1.4	1.4
Chang *et al.* [16]	0	0	$\varepsilon_w = \nu\left(\frac{\partial^2 k}{\partial y^2}\right)$	0.09	1.44	1.92	1.0	1.3

did our modified model (CHC model, [16]). It is interesting to note that both the AKN and the NT models adopted different values of the turbulence model constants such as C_1, C_2, σ_k and σ_ε, as shown in Table 3, from those conventionally used for the standard k-ε model. Furthermore, even the AKN model used different values of some turbulence model constants from those of its predecessor (the NT model). The NT model adjusted the values of the turbulence model constants for best fitting experimental data in straight-pipe flow [15], while the AKN model adjusted these values to obtain better prediction of the reattachment length of a backward-facing step flow [18]. This implies that their turbulence model constants are case-dependent. In contrast to the AKN model, our modified (CHC) model and the YS model use the same values of the turbulence model constants as those conventionally used for the standard k-ε model (see Table 3).

MATHEMATICAL FORMULATION AND NUMERICAL ANALYSIS

Two experimental studies of axisymmetrical, non-isothermal sudden-expansion flows are selected as the test problems in this work. One is the case with uniform wall temperature condition conducted by Baughn *et al.* [25]. The other is the case with uniform wall heat flux condition conducted by Zemanick and Dougall [26].

Governing equations

The present work deals with steady-state, axisymmetric, Reynolds-averaged equations for conservation of momentum, energy, turbulent kinetic energy and energy dissipation rate. These governing equations are cast into the following general form which permits a single algorithm to be used:

$$\frac{1}{r}\left[\frac{\partial}{\partial x}(r\rho u\theta) + \frac{\partial}{\partial r}(r\rho v\theta)\right] = \frac{1}{r}\left[\frac{\partial}{\partial x}\left(r\Gamma_\theta \frac{\partial \theta}{\partial x}\right) + \frac{\partial}{\partial r}\left(r\Gamma_\theta \frac{\partial \theta}{\partial r}\right)\right] + S_\theta. \quad (13)$$

The parameters θ, Γ_θ and S_θ appearing in equation (13) are summarized in Table 2. The corresponding model constants and functions shown in Table 2 for each tested turbulence model are listed in Table 3 for the reader's convenience.

Numerical solution procedures

There are no significant differences between the current numerical solution procedure and the earlier one [16]. Therefore, the employed numerical solution procedure is briefly described here.

The finite-volume method incorporated with the power-law scheme and the SIMPLER algorithm [27] is used to solve numerically the partial differential equations summarized in Table 2. One may argue that numerical (or false) diffusion can be introduced through the discretization of the governing equations,

particularly for the problem in complex flows with stream-to-grid skewness. The use of high-order numerical schemes can, to a certain degree, reduce the numerical diffusion. However, the use of high-order numerical schemes sometimes aggravates the numerical instability.

In order to reduce the numerical diffusion of the investigated recirculating flow by use of the power-law scheme, care must be taken in establishing the grid meshes. Distribution of the grid nodes must be done to ensure that the small regions that exert a large influence on the flow field are adequately resolved. Grid meshes used for the computational domains for both tested flows consist of 70×90 nonuniformly distributed nodes. Numerical tests disclosed that these nonuniform grid meshes yielded nearly grid-independent solutions for all investigated flow cases, as compared to the solution obtained with the denser grid meshes of 85×110. It is reported [28] that the grid nodes below the inertia sublayer ($y^+ < 30$) are very sensitive to the predictions of wall heat/mass transfer rate. For those models which do not exhibit the proper near-wall limiting behavior of $f_\mu \propto y^{+3}$, the first grid node could be placed as close as $y^+ = 0.1$. However, the choice of the position of the first grid node for those models possessing the proper near-wall limiting behaviors must be careful, otherwise it may result in an unrealistic value of $f_\mu > 1$. It is found that the solution is not very sensitive to the near-wall grid distributions as long as the first grid node is placed at $y^+ \simeq 2$ for the models possessing the proper near-wall limiting behavoirs investigated in this work. The convergence criterion adopted in the present work is that the summation of the absolute mass residuals normalized by the inlet mass, in the entire computational domain, is less than 10^{-7}.

RESULTS AND DISCUSSION

Uniform wall temperature case

The diameters of the upstream (d) and downstream (D) tubes were 38.1 and 95.3 mm, respectively, to achieve a 2.5 expansion ratio (ERP = D/d) in the experimental work of Baughn *et al.* [25]. The test chamber had a total length of 16 D. The Reynolds number based on the mean flow velocity at the inlet was 17 300. Temperature measurements were made by three different means: a hot wire probe, a chrome-constantan thermocouple probe and a miniature thermistor. Velocity measurements were made by a single hot wire probe along with a TSI-1050 anemometer. However, as pointed out by Baughn *et al.* [25], the single hot wire was unable to resolve flow direction and was thus unable to provide confident velocity information in the recirculating zone.

In the experiment of Baughn *et al.* [25], no measurements were provided for the inlet region. However, they reported that a fully-developed profile of mean velocity and low level turbulence intensity were observed in the inlet region because the upstream tube was sufficiently long (48 d). Thus, the mean axial velocity profile was assumed using the one-seventh law at the inlet [6]. The mean radial velocity component at the inlet was set to be zero. The inlet profiles for k and ε were given in the following empirical manner [9]:

$$k = 0.003u^2 \tag{14}$$

$$\varepsilon = C_\mu^{1.5}/0.03R. \tag{15}$$

It was reported [29] that the employment of the assumed inlet profiles of k and ε did not significantly influence flowfield calculations for geometries like that presently investigated, except in the very near-inlet region and in the presence of high turbulence intensity. A uniform mean temperature of 300 K was specified at the inlet in the absence of better information. Note that the physical domain had a length of 16 D. Numerical tests revealed that no significant axial variations from velocity components were found at the axial positions after the station of $x/D = 9.0$. Thus, the outlet boundary of computational domain was chosen at the axial distance of $x/D = 9.0$, and the outlet boundary was reasonably assumed to be fully developed in the calculation. At the bounded wall, all quantities vanished, except for T_w which had been prescribed in the experiment of Baughn *et al.* [25] and for ε_w which is given in Table 3. At the symmetric axis, the condition of zero gradient, $\partial\theta/\partial r = 0$, was met except for the radial velocity component which is naturally zero.

Figure 1 shows a comparison of the predicted and the measured distributions of the Nusselt number along the wall using all investigated models except the AKN and YS models. Clearly, only one model, the CHC model, is capable of giving correct trends. The models which do not exhibit the near-wall limiting behaviors, such as the LS and LB models, tend to significantly overpredict the values of the Nusselt number in the regions around the reattachment points. A tendency similar to that presented in Fig. 1 has recently been found in wall mass transfer problems with the same group of the low-Reynolds-number k-ε

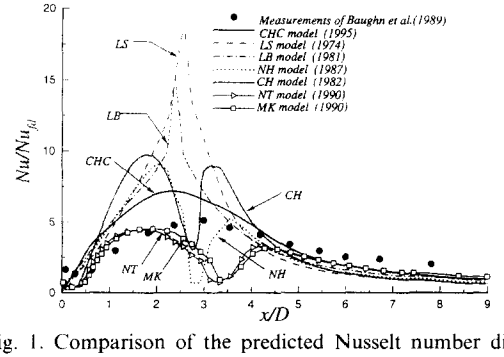

Fig. 1. Comparison of the predicted Nusselt number distributions obtained through various low-Reynolds-number models with the measurements (Re = 17 300 and EPR = 2.5).

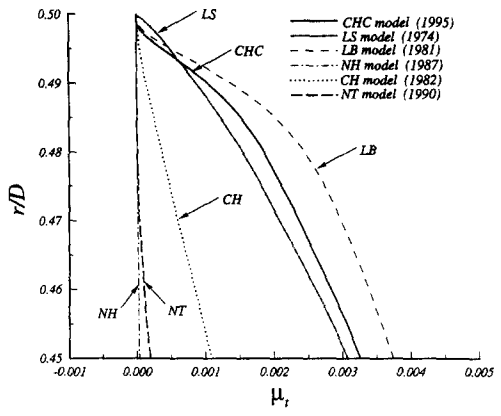

Fig. 2. Comparison of the near-wall profiles of eddy viscosity obtained through various low-Reynolds-number k-ε models in the sections of reattachment points (Re = 17 300 and EPR = 2.5).

models [28, 30]. That is, as shown in Fig. 2, over-predicting μ_t value results in an excessively high wall heat transfer rate in the vicinity of the reattachment point. Models which have the singular problems, such as the MK and NT models, tend to underpredict the values of the Nusselt number, particularly in the regions around the reattachment point. Nevertheless, it is generally known that the maximum wall heat transfer rate occurs in the vicinity of the reattachment points. Thus, the application of models with the singularity defect in the flows in pipe-expansion geometries would yield unrealistic predictions of the wall heat transfer rate. Accordingly, of all the models investigated, the CH and NH models, which possess both of the aforementioned defects, are least likely to yield correct predictions. Their predicted distributions of the Nusselt number (see Fig. 1) show combined effects which stem from the two defects mentioned here.

Figure 2 shows the near-wall profiles of the eddy viscosity (μ_t) obtained in the sections of the reattachment points for the investigated low-Reynolds-number k-ε models. Note that in flow calculations, the reattachment lengths vary with each model. The following results with regard to the reattachment points were interpolated in the results obtained in the front and back consecutive grid lines. It is clearly revealed in Fig. 2 that the LS and LB models do not possess the near-wall limiting behavior of μ_t as does our modified (CHC) model, and that the predicted μ_t profile obtained with the LS model is very singular to that obtained with the CHC model, except in the near-wall region. Nevertheless, this small difference leads to a tremendous change of Nusselt number predictions, as shown in Fig. 1. Those models which have similar problems incorrectly underpredicted μ_t values in comparison to the CHC model.

The predicted profiles of the mean temperatures, obtained through four respective low-Reynolds-number k-ε models, including the LS (without near-wall limiting behavior), NT (with singularity difficulty), NH (with both the defects), and CHC models, at

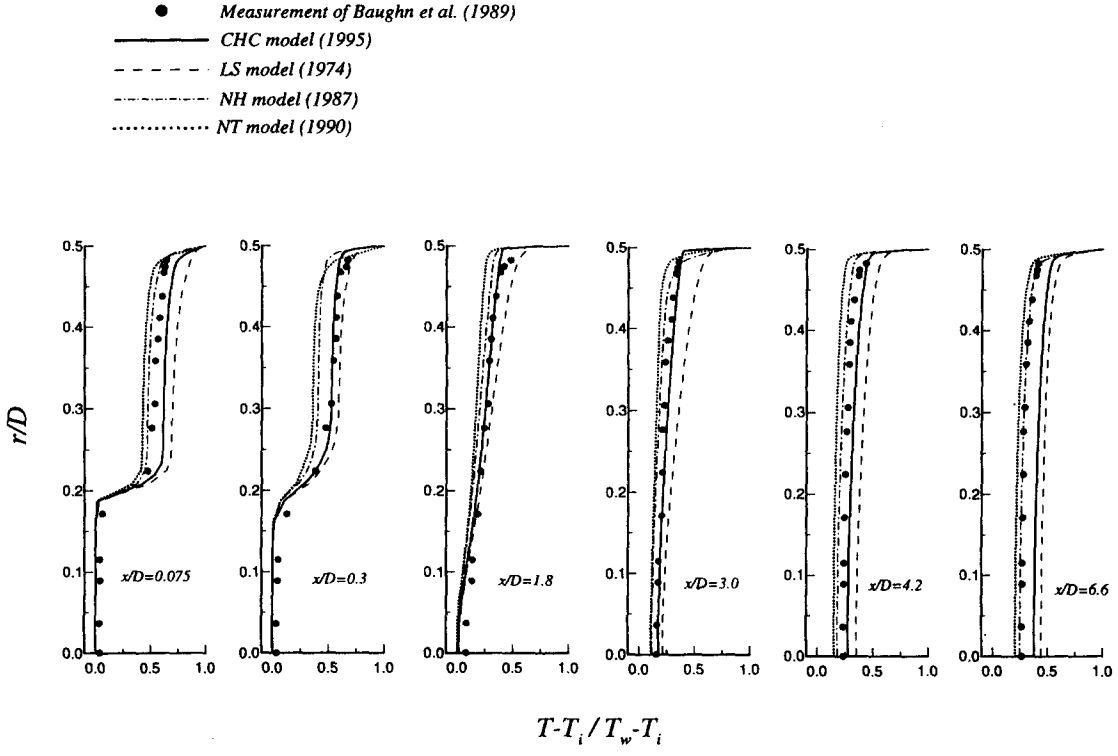

Fig. 3. Comparison of the predicted mean temperature profiles obtained through some investigated low-Reynolds-number models with the measurements at various stations (Re = 17 300 and EPR = 2.5).

various axial stations are presented in Fig. 3, respectively, along with the measured data Baughn *et al.* [25]. Figure 3 shows that the CHC model yields the best performance of the four models investigated. A similar study for mean axial velocity has also been done. Since the maximum difference between the wall (heated) temperature and the air (room) temperature is about 10 K in the experiment of Baughn *et al.* [25], the mean velocity field, therefore, differs slightly from that of the isothermal case which has been extensively investigated in our previous work [16]. For the sake of brevity, the comparative results will not be presented here. However, the same conclusions as that expressed in Fig. 3 can be drawn; that is, of the four models investigated, the CHC model has the best performance for velocity simulation.

As mentioned previously, both the CHC, AKN and YS models are free of the singularity difficulty near the reattachment point. Among them, the CHC and AKN models can exhibit the proper near-wall limiting behaviors. Although the YS model does not give the proper near-wall limiting behavior, it introduces the Kolmogorov time scale into the μ_t calculation to account for this defect. These three models were then selected for comparison with experimental data in order to better understand their performances. The predicted profiles of mean velocity and mean temperature at various axial stations, as obtained through the CHC, AKN and YS models, are presented in Fig. 4 and compared with the measured data of Baughn *et al.* [25]. Note that, as Baughn *et al.* [25] admitted, we cannot be confident of the measured velocity data within the recirculation zone due to the limitation of the measurement instruments used in their experiment. Figure 5 shows three predicted distributions of the Nusselt number along the wall, as obtained through these three models, in comparison with the experimental data. Clearly, the YS model performed

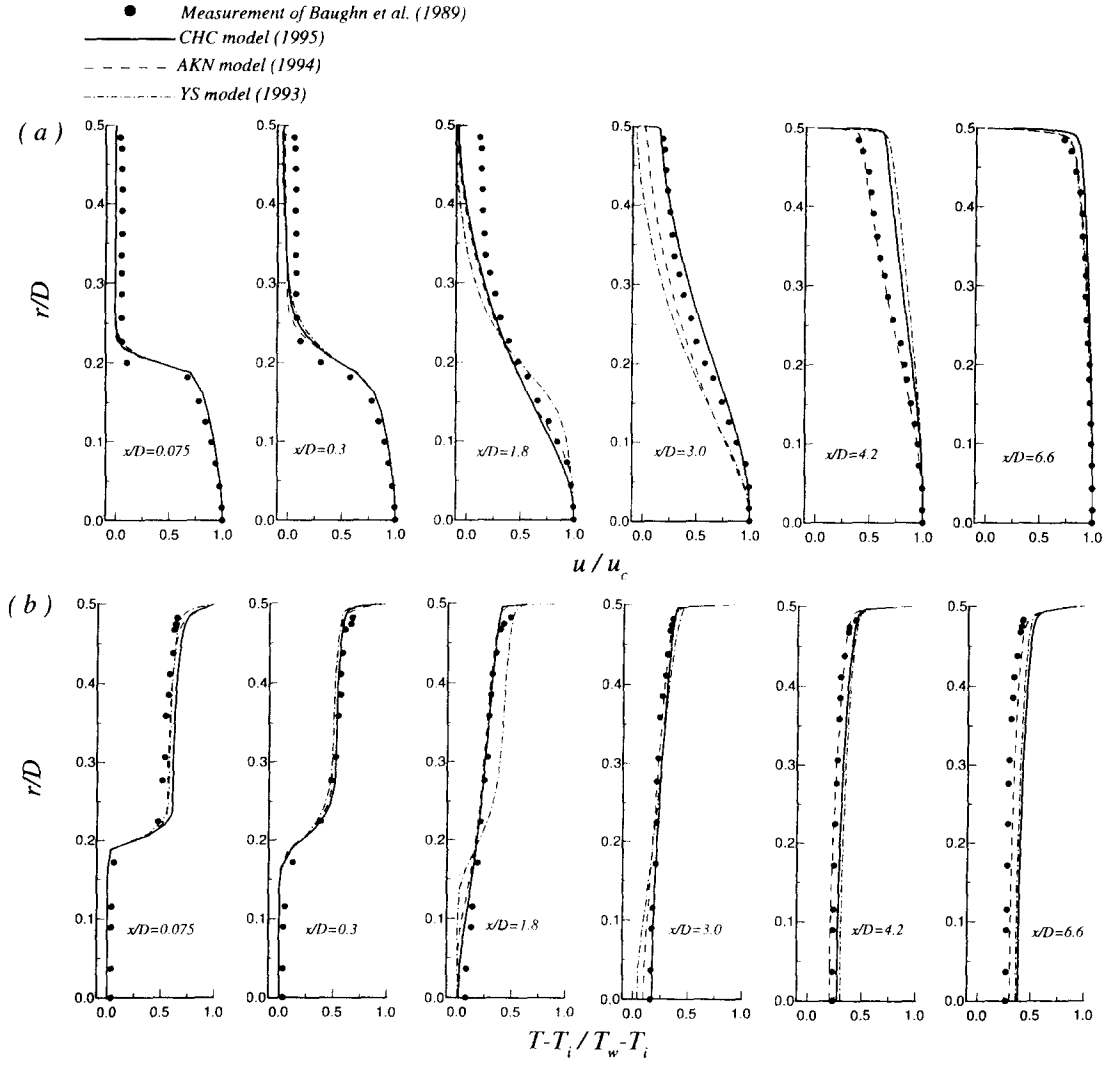

Fig. 4. Comparison of the predicted (a) mean velocity profiles and (b) mean temperature profiles obtained through the CHC, AKN and YS models with the measurements at various stations (Re = 17300 and EPR = 2.5).

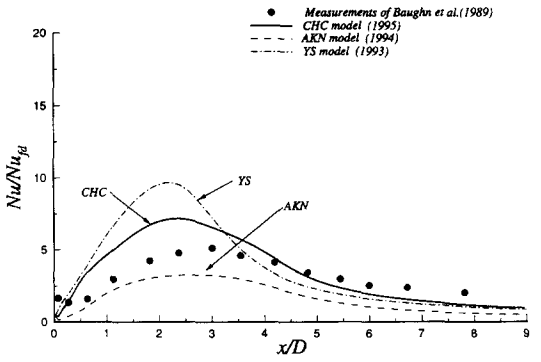

Fig. 5. Comparison of the predicted Nusselt number distributions obtained through the CHC, AKN and YS models with the measurements (Re = 17 300 and EPR = 2.5).

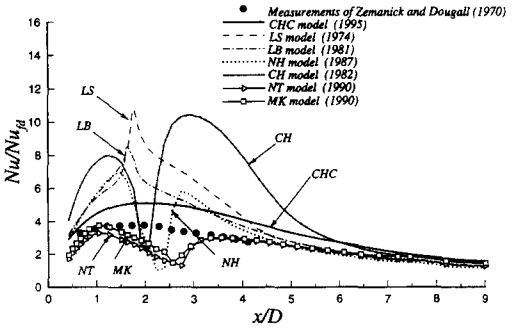

Fig. 6. Comparison of the predicted Nusselt number distributions obtained through various low-Reynolds-number models with the measurements (Re = 48 090 and EPR = 1.86).

worst among these three models in the predictions presented in Figs. 4 and 5. Nevertheless, it does not yield a peculiar overshoot in Nu predictions as did the LS and LB models, which do not exhibit the near-wall limiting behaviors, Fig. 1. Both of the CHC and AKN models seem to give reasonable predictions, as a comparison of Figs. 4 and 5 shows. Thus, it is difficult to tell which one of the CHC and AKN models performs better in this problem with uniform wall temperature. It should be pointed out that, as mentioned previously, the turbulence model constants of the AKN model differ from those conventionally used for the standard k-ε model (see Table 3).

Uniform wall heat flux case

The diameters of the upstream (d) and downstream (D) tubes were 12.7 and 23.6 mm, respectively, to achieve a 1.86 expansion ratio in the experimental work of Zemanick and Dougall [26]. Two cases with Reynolds numbers of 48 090 and 9620 were tested in this study. Wall and bulk temperatures were measured using thermocouples. Measurements of velocity distribution was not implemented in this experimental work.

Again, no measured data were provided for the inlet region in the experiment. The same inlet and boundary conditions as described fro the previous test problem, with the exception that uniform wall temperature is replaced by uniform wall heat flux, are used for the following calculations.

Figure 6 compares the predicted and the measured distributions of the Nusselt number using all investigated models except the AKN and YS models along the wall for Re = 48 090. Once again, the results were similar to those discussed previously in the first (uniform wall temperature) test problem. In other words, of the seven models investigated, CHC is the only model which can give correct trend.

Comparisons of the predicted distributions of the Nusselt number obtained through the CHC, AKN and YS models for two test cases with different Reynolds numbers are plotted in Fig. 7. Once more, the YS model performs worst among these three models.

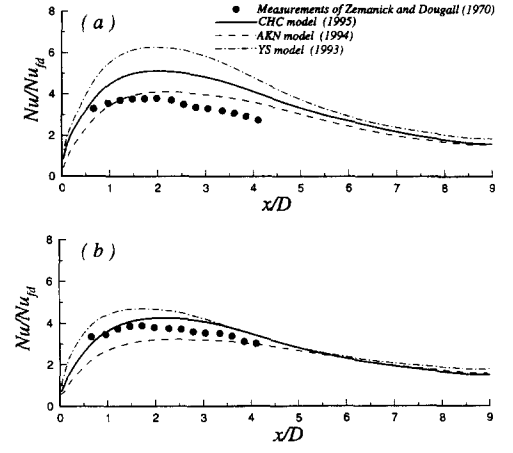

Fig. 7. Comparison of the predicted Nusselt number distributions obtained through the CHC, AKN and YS models with the measurements for the cases of (a) Re = 48 090 and (b) Re = 9620 (EPR = 1.86).

The predicted trends obtained by the CHC and AKN models are in fair agreement with the measurements for both the test cases. It is still hard to tell which one of the CHC and AKN models perform better in the problem with uniform wall heat flux, because the AKN model yields better predictions of Nu distribution in the case of Re = 48 090 [see Fig. 7(a)], while the CHC model does so in the case of Re = 9620 [see Fig. 7(b)].

CONCLUSIONS

The predictions of nine low-Reynolds-number k-ε turbulence models have been examined in regard to heat transfer problems occurring in pipe flows with sudden-expansion geometry. Two different problems with the boundary conditions of (1) uniform wall temperature and (2) uniform wall heat flux were tested. The corresponding experimental data, collected from the open literature, were used as a base for model comparisons.

It was found that all the investigated conventional low-Reynolds-number k-ε models, which are subject

to the defect of either lack of near-wall limiting behavior or the existence of singularity difficulty, fail to yield correct predictions of the wall heat transfer rate. Two currently developed low-Reynolds-number k-ε models, i.e. the CHC and AKN models, which are free of both defects mentioned above are shown to be capable of yielding the reasonable trend of the distribution of the Nusselt number among the tested models. However, the turbulence model constants adopted by the CHC model are the same as those conventionally used for the standard k-ε model, and CHC model is thus more universal than the AKN model.

Acknowledgements—The authors gratefully acknowledge the grant support from the National Science Council of the Republic of China for this work under the contract NSC83-0424-E006-094.

REFERENCES

1. C. C. Chieng and B. E. Launder, On the calculation of turbulent heat transfer downstream from an abrupt pipe expansion, *Numer. Heat Transfer* **3,** 189–207 (1980).
2. R. S. Amano, A study of turbulent flow downstream of an abrupt pipe expansion, *AIAA J.* **21,** 1400–1405 (1983).
3. R. S. Amano, Development of a turbulent near-wall model and its application to separate and reattached flows, *Numer. Heat Transfer* **7,** 59–75 (1984).
4. A. M. Gooray, C. B. Watkins and W. Aung, Turbulent heat transfer computations for rearward-facing steps and sudden pipe expansions, *ASME J. Heat Transfer* **107,** 70–76 (1985).
5. M. Prud'homme and S. Elghobashi, Turbulent heat transfer near the reattachment of flow downstream of a sudden expansion, *Numer. Heat Transfer* **10,** 349–386 (1986).
6. C. Yap, Turbulent heat and momentum in recirculating and impinging flows, Ph. D. thesis, University of Manchester, Institute of Science and Technology, Manchester (1987).
7. S. Jakrlić and K. Hanjalić, On the performance of the second-moment high- and low-renumber closure in reattaching flows, *Proceedings of the International Symposium on Turbulence and Heat Mass Transfer*, Vol. 1, pp. 3.2.1–3.2.6, Lisbon, Portugal (1994).
8. B. E. Launder, Second-moment closure: present ... and future?, *Int. J. Heat Mass Transfer* **10,** 282–300 (1989).
9. M. Nallasamy, Turbulence models and their applications to the prediction of internal flows: a review, *Comput. Fluids* **3,** 151–194 (1987).
10. P. A. Durbin, Application of a near-wall turbulence model to boundary layers and heat transfer, *Int. J. Heat Fluid Flow* **14,** 316–323 (1993).
11. S. Dutta and S. Acharya, Heat transfer and flow past a backstep with the nonlinear k-ε turbulence model and the modified k-ε model, *Numer. Heat Transfer A* **23,** 281–301 (1993).
12. H. K. Myong, Numerical investigations of fully developed turbulent fluid flow and heat transfer in a square duct, *Int. J. Heat Fluid Flow* **12,** 344–352 (1991).
13. V.C. Patel, W. Rodi and G. Scheuerer, Turbulence models for near-wall and low-Reynolds-number flows: a review, *AIAA J.* **23,** 1308–1319 (1985).
14. H. K. Myong and N. Kasagi, A new approach to improved of k-ε turbulence model for wall-bounded shear flows, *JSME J. Ser. II* **33,** 63–72 (1990).
15. Y. Nagano and M. Tagawa, An improved k-ε model for boundary layer flows, *ASME J. Fluids Engng* **112,** 33–39 (1990).
16. K. C. Chang, W. D. Hsieh and C. S. Chen, A modified low-Reynolds-number turbulence model applicable to recirculating flow in pipe expansion, *ASME J. Fluids Engng* **117,** 417–423 (1995).
17. Z. Yang and H. T. Shih, New time scale based k-ε model for near-wall turbulence, *AIAA J.* **31,** 1191–1198 (1993).
18. K. Abe, T. Kondoh and Y. Nagano, A new turbulence model for predicting fluid flow and heat transfer in separating and reattaching flows—I. Flow field calculations, *Int. J. Heat Mass Transfer* **37,** 139–151 (1994).
19. B. E. Launder and B. I. Sharma, Application of the energy-dissipation model of turbulence to the calculation of flow near a spinning disc, *Lett. Heat Mass Transfer* **1,** 131–138 (1974).
20. C. K. G. Lam and K. A. Bremhorst, Modified form of the k-ε model for predicting wall turbulence, *ASME J. Fluids Engng* **103,** 456–460 (1981).
21. K. Y. Chien, Prediction of channel and boundary-layer flows with a low-Reynolds-number turbulence model, *AIAA J.* **20,** 33–38 (1982).
22. Y. Nagano and M. Hishida, Improved form of k-ε model for wall turbulent shear flows, *ASME J. Fluids Engng* **109,** 156–160 (1987).
23. T. H. Shih and J. L. Lumley, Kolmogorov behavior of near-wall turbulence and its application in turbulence modeling, *Int. J. Comput. Fluid Dyn.* **1,** 43–56 (1993).
24. S. Fan, B. Lakshminarayana and M. Barnett, Low-Reynolds-number k-ε model for unsteady turbulent boundary-layer flows, *AIAA J.* **31,** 1777–1784 (1993).
25. J. W. Baughn, M. A. Hoffman, B. E. Launder, R. K. Takahashi and C. Yap, Heat transfer, temperature, and velocity measurements downstream of an abrupt expansion in a circular tube at a uniform wall temperature, *ASME J. Heat Transfer* **111,** 870–876 (1989).
26. P. P. Zemanick and R. S. Dougall, Local heat transfer downstream of abrupt circular channel expansion, *ASME J. Heat Transfer* **92,** 53–60 (1970).
27. S. V. Patankar, *Numerical Heat Transfer and Fluid Flow*. Hemisphere, Washington, DC (1980).
28. J. Herrero, F. X. Grau, J. Grifoll and F. Giralt, The effect of grid size in near-wall k-ε calculations of mass transfer rates at high Schmidt numbers, *Int. J. Heat Mass Transfer* **37,** 882–884 (1994)
29. M. Nallasamy and C. P. Chen, Studies on effects of boundary conditions in confined turbulent flow predictions, NASA CR-3929 (1985).
30. S. Nešić, J. Postlethwaite and D. J. Bergstorm, Calculations of wall-mass transfer rates in separated aqueous flow using a low Reynolds number k-ε model, *Int. J. Heat Mass Transfer* **35,** 1977–1985 (1992)